Bulletin of the Seismological Society of America. Vol. 56, No. 3, pp. 733–747. June, 1966

PP AND CRUSTAL STRUCTURE

By Francis T. Wu and W. J. Hannon

ABSTRACT

Haskell's formulation for reflection of *P* waves at the base of a solid crust is extended to include overlying liquid layers. Normalized displacement and the phase shift at the base of the crust as a function of angle of incidence and frequency are calculated for two continental models and an oceanic model. Complex reflection coefficients are inverse Fourier transformed to the time domain to show the change of pulse shape upon reflection. These time traces show that the water layer of the oceanic model causes the main difference between continental and oceanic reflections. Sample seismograms from a deep shock were compared to the theoretical records; they were found to be consistent. It is concluded that the amplitude ratio *PP/P* as a function of frequency obtained from seismograms can be used to decipher the detailed structure at the point of reflection only after the radiation pattern of the source, attenuation of waves during propagation, and crustal transmission response at the receiver are properly taken into account.

Introduction

The effect of the crust on the reflected compressional wave PP has been studied extensively by Gutenberg and Richter (1935), Mei (1943), Byerly *et al* (1949), and Papazachos (1964). Most of the quantitative work in these studies has involved determination of the amplitude ratio PP/P or the variation in the angle of incidence. Although Gutenberg and Richter attempted to investigate the differences in crustal structure beneath the Atlantic and Pacific Oceans using the amplitude ratio PP/P, others (Byerly *et al*, 1949; Ben Menahem *et al*, 1965) have indicated that the fluctuation of this ratio could result from the radiation pattern of the source rather than the crustal structure at the point of reflection. In any event, a great deal of information is lost in any investigation using only the maximum amplitudes of the pulse.

In order to provide a more sensitive measure of the crustal effect at the receiver, frequency dependent reflection coefficients have been computed for several typical oceanic and continental crustal models for frequencies less than 0.45 cps. Using these coefficients and the transmission coefficients for a central U. S. crustal structure, waveforms are synthesized and compared to seismograms from the Banda Sea earthquake of March 21, 1964. The synthesized wave forms exhibit many of the properties found on the actual seismograms.

Method of Computation

In order to obtain some measure of the effect of crustal layering on reflected waves such as PP, it is convenient to consider a crustal model composed of plane parallel layers. If the incident wave is represented as a plane wave, then the frequency response of a model of this type, both in transmission and reflection, may be determined by the Haskell-Thomson matrix method (Haskell, 1953, 1960, 1962;

Thomson, 1950). The theory has been discussed in the works of Haskell and Thomson above, and in papers by Dorman (1962) and Harkrider (1964b). Although the discussions of layered systems involving liquid layers are quite general in the works of Dorman and Harkrider, the techniques considered are oriented toward surface waves. Since there are some aspects of the matrix formulation which are of particular interest when a model of an oceanic structure is considered, a brief development of the theory for a layered system consisting of liquid layers overlying solid layers will be presented here.

In a system of n layers (Figure 1) let the upper $r(r < n)$ layers be liquid and the remaining layers be solid. The horizontal motion at the fluid-solid interface is decoupled and the tangential stress vanishes. Then the relations among the horizontal particle velocity at the liquid-solid interface, the vertical particle velocity at the free surface and the dilatations and rotations in the half-space may be expressed as

$$\begin{bmatrix} \Delta_n' + \Delta_n'' \\ \Delta_n' - \Delta_n'' \\ \omega_n' - \omega_n'' \\ \omega_n' + \omega_n'' \end{bmatrix} = E_n^{-1} A_{n-1} \cdots A_{r+1} A F_r \cdots A F_1 \begin{bmatrix} \frac{\dot{u}_r}{c} \\ \frac{\dot{w}_0}{c} \\ 0 \\ 0 \end{bmatrix} \tag{1}$$

where:

(1) E_n^{-1} and $A_i (i = r + 1, n - 1)$ are the standard (Haskell, 1953) 4×4 layer matrices for the solid layers

(2) $\dot{u}_r$ is the horizontal component of the particle velocity at the top of the $r + 1$ layer (that is the top of the solid section)

(3) $\dot{w}_0$ is the vertical component of the particle velocity at the free surface

(4) AF_j $(j = 1, r)$ is a 4×4 matrix of the form of Haskell (1953 equation 6.3) with the following modifications

a) $(AF_j)_{11} = 1$

b) $(AF_j)_{1k} = 0, k = 2, 4$

(5) Δ_n and ω_n are the amplitudes of the dilatations and rotations in the half space. The single primes represent down going waves and the double primes represent up going (incident) waves.

(6) c is the apparent surface velocity.

If we let $E_n^{-1} A_{n-1} \cdots A_{r+1} A F_r \cdots A F_1 = J_1$ then the four equations arising from 1) may be solved for Δ_n'', ω_n'', $\dot{u}_r/c$, and $\dot{w}_0/c$, as in Haskell (1962 eq. 3-6, 12-15) with the substitution of $\dot{u}_r/c$ for $\dot{u}_0/c$.

With these results, we have the amplitudes of the reflected dilatations and rotations, i.e., waves of the types PP and PS or SP and SS depending on the type of incident wave. In addition, we have horizontal components of velocity at the top of the solid layer, and the vertical component of velocity at the free surface. In order to obtain the vertical component at the top of the solid system (with a view toward application in ocean bottom observations), we can use the relation

$$\begin{bmatrix} \frac{\dot{u}_r}{c} \\ \frac{\dot{w}_r}{c} \\ \sigma_r \\ \tau_r \end{bmatrix} = AF_r \cdots AF_1 \begin{bmatrix} \frac{\dot{u}_r}{c} \\ \frac{\dot{w}_0}{c} \\ 0 \\ 0 \end{bmatrix}. \tag{2}$$

If we let $AF_r \cdots AF_1 = S$, then the four equations obtained from (2) may be written

$$\frac{\dot{u}_r}{c} = S_{11} \frac{\dot{u}_r}{c} + S_{12} \frac{\dot{w}_0}{c} \tag{3}$$

$$\frac{\dot{w}_r}{c} = S_{21} \frac{\dot{u}_r}{c} + S_{22} \frac{\dot{w}_0}{c} \tag{4}$$

$$\sigma_r = S_{31} \frac{\dot{u}_r}{c} + S_{32} \frac{\dot{w}_0}{c} \tag{5}$$

$$\tau_r = S_{41} \frac{\dot{u}_r}{c} + S_{42} \frac{\dot{w}_0}{c}. \tag{6}$$

From the properties of the matrices AF described above and in Haskell (1953) it is readily seen that

$$S_{1j} = S_{j1} = 0 \qquad j = 2, 4$$

and

$$S_{11} = 1.$$

Thus equations (3)–(6) may be written

$$\frac{\dot{u}_r}{c} = \frac{\dot{u}_r}{c} \tag{7}$$

$$\frac{\dot{w}_r}{c} = S_{22} \frac{\dot{w}_0}{c} \tag{8}$$

$$\sigma_r = S_{32} \frac{\dot{w}_0}{c} \tag{9}$$

$$\tau_r = 0. \tag{10}$$

These equations, when combined with those previously given by Haskell (1953, 1962) allow us to obtain the motion reflected from an oceanic crustal structure as well as the motion occurring at the ocean bottom.

In order to show the effect of crust on reflected pulses at the bottom of the crust we have synthesized the complex Fourier spectrums for several models and angles of incidence using the following formula which was first discussed by Aki (1960) and subsequently extended by Harkrider (1964a):

$$h(t) = \sum_i \int_{\omega_i-(\Delta\omega_i/2)}^{\omega_i+(\Delta\omega_i/2)} \bar{A}(\omega) \cos \phi(\omega)\, d\omega$$

$$= 2 \sum_i \left\{ \bar{A}_i \Delta\omega_i \cos \omega_i(t - \tau_i) \frac{\sin\left[\frac{\Delta\omega_i}{2}(t - t_{gi})\right]}{\left[\frac{\Delta\omega_i}{2}(t - t_{gi})\right]} \right.$$

$$\left. - \left(\frac{\partial \bar{A}}{\partial \omega}\right)_i \Delta\omega_i \frac{\sin \omega_i(t - \tau_i)}{(t - t_{gi})} \left[\frac{\sin\left[\frac{\Delta\omega_i}{2}(t - t_{gi})\right]}{\left[\frac{\Delta\omega_i}{2}(t - t_{gi})\right]} - \cos\left[\frac{\Delta\omega_i}{2}(t - t_{gi})\right] \right] \right\}$$

$h(t)$ = the synthesized waveform
$\bar{A}(\omega)$ = amplitude spectrum
$\phi(\omega)$ = phase spectrum
τ_i = phase delay
t_{gi} = group delay
ω_i = frequency
$\Delta\omega_i$ = frequency increment.

Results of Computation

Contour Maps of Reflection Coefficients. Three crustal models were chosen to show the effects of crustal structures on the variations of reflection coefficients as a function of angle of incidence and frequency. The three models are: (1) average oceanic structure (Raitt, 1963), (2) Peru-Altiplano (Steinhart and Meyer, 1961), and (3) central U. S. average crust (McEvilly, 1964). They are listed in Table 1. No attempt was made to differentiate Atlantic and Pacific crusts as they are not significantly different from each other (Raitt, 1963).

The ocean depth in the average oceanic structure mentioned above is 4.5 km. As we shall see later this depth affects the reflected pulse in a rather interesting way; we have changed the depth to 3 km and 2 km to demonstrate its effect on the synthesized waveform.

For each of these models, reflection coefficients at the bottom of the crust are calculated for angles of incidence ranging from 0 to 90 degrees at $\frac{1}{2}$ degree intervals and for frequencies from 0 to 0.45 cps, at 0.003 cps intervals. These are on-line contoured by the IBM 7094 computer. Figures 2–4 contain the amplitude response of the reflected P wave for the three models just mentioned. Figures 5 and 6 contain the phase shift contours for central U. S. crust and average oceanic crust respectively. It is clear that for very low frequency the reflection coefficients approach those calculated by Gutenberg (1944) and Brekhovskikh (1960).

As frequency increases the behavior of the coefficients begin to have significant differences. Thus, interpreting PP/P ratios which have been observed with different instruments or at different distances under the assumption of a homogeneous half-space at the reflection point may yield results that are devoid of meaning.

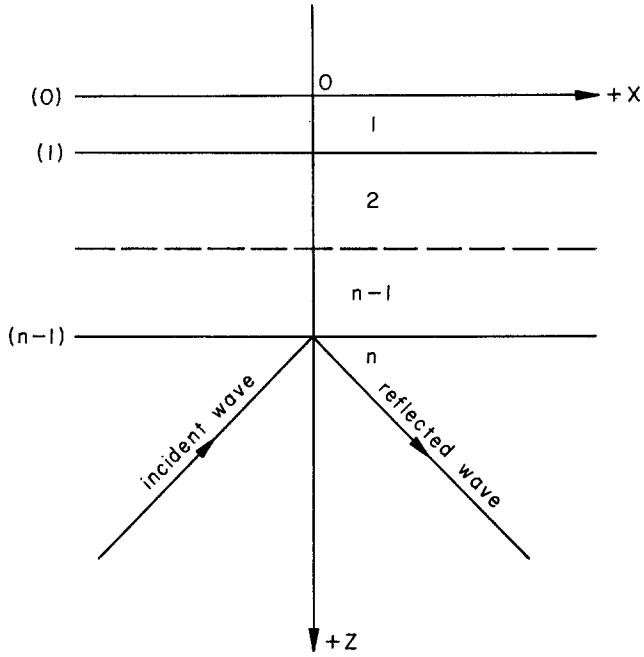

FIG. 1. Geometry of the problem and numbering of layers and interfaces.

TABLE 1

CRUSTAL MODELS USED IN THE COMPUTATIONS

	Average Oceanic				Peru-Altiplano				Central U. S.			
	d	α	β	ρ	d	α	β	ρ	d	α	β	ρ
Top layer..	4.50	1.50	0	1.03	4.1	5.3	3.0	2.40	11.0	6.10	3.50	2.70
2nd layer...	0.45	2.0	1.0	1.70	21.2	6.2	3.59	2.80	9.0	6.40	3.68	2.90
3rd layer...	1.75	5.0	2.88	2.30	39.6	6.70	3.94	2.90	18.0	6.70	3.94	2.90
4th layer...	4.70	6.71	3.86	2.84								
Half-space..	∞	8.09	4.65	3.25	∞	8.0	4.70	3.25	∞	8.15	4.75	3.30

d = layer thickness, α = P wave vel., β = S wave vel., ρ = density.

It might be proper to mention here that differential attenuation of seismic waves with respect to frequency would also render incoherent the amplitude ratio PP/P measured on seismograms recorded by instruments having different response.

For PP waves the middle portion of the contour map with angle of incidence between 20° and 55° is of interest, while for pP the smaller angles of incidence are pertinent. However, in dealing with pP, consideration has to be given to the curva-

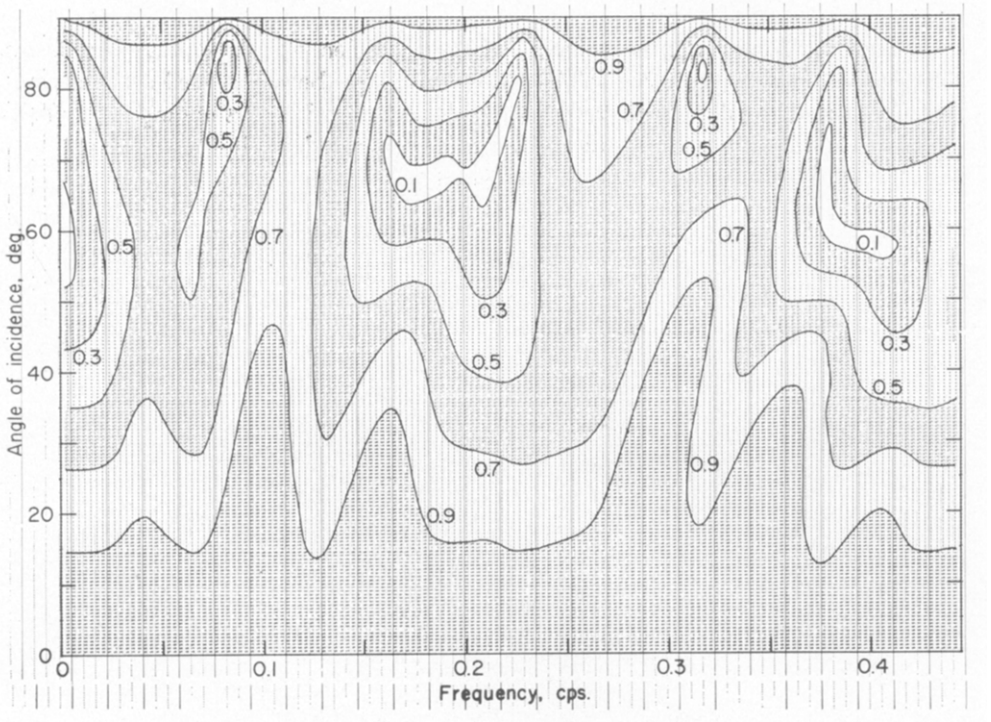

FIG. 2. Normalized P wave displacement at the base of the crust $|\Delta'/\Delta''|$, for average central U. S. structure.

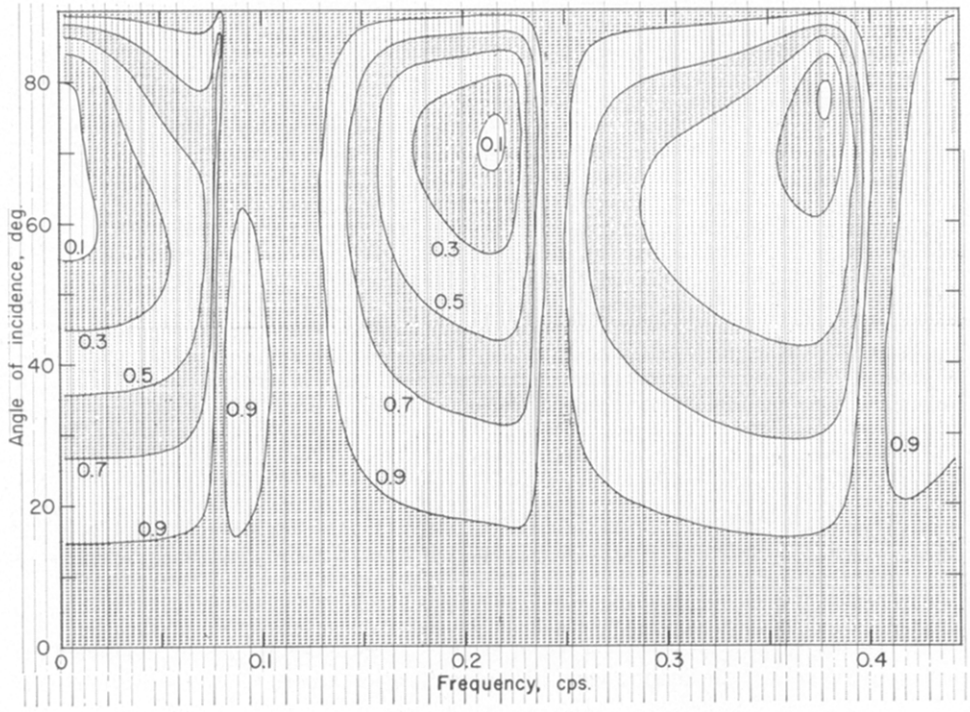

FIG. 3. Normalized P wave displacement at the base of the crust $|\Delta'/\Delta''|$, for average oceanic structure.

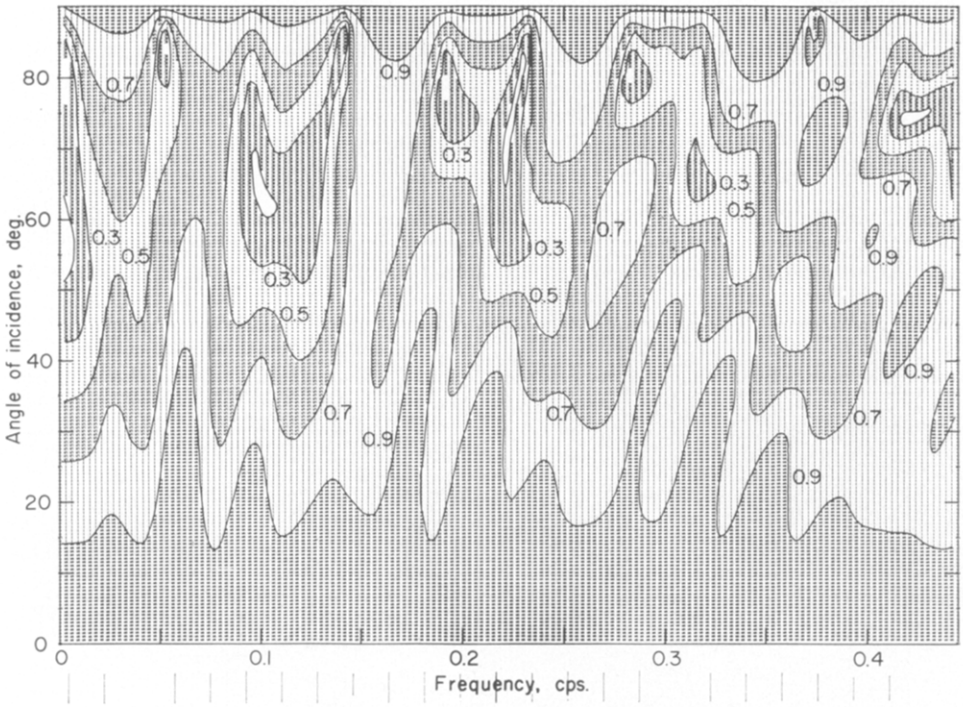

FIG. 4. Normalized P wave displacement at the base of the crust $|\Delta'/\Delta''|$, for Peru-Altiplano structure.

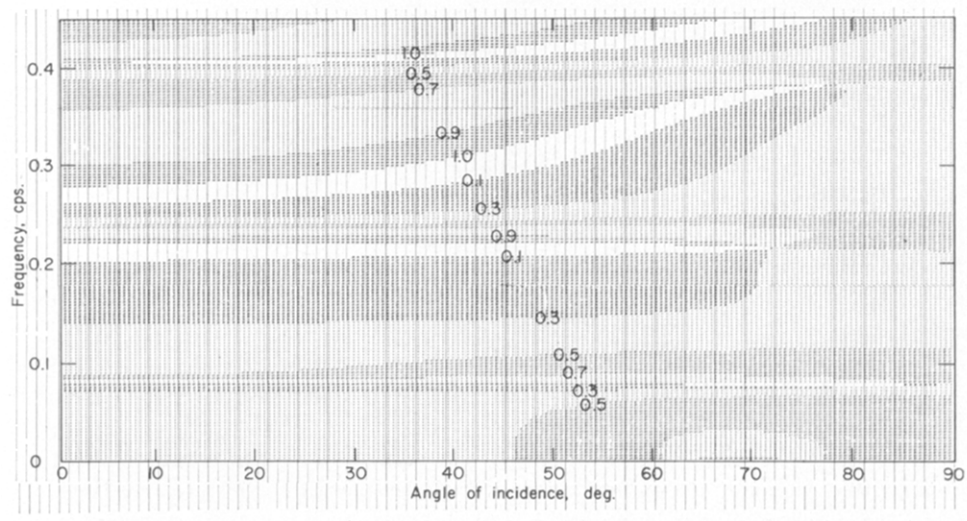

FIG. 5. Phase shift (fraction of a circle) at the base of the crust for average oceanic structure.

ture of the wave front, as the distance between the source and the reflector is usually small for the wavelength concerned, and the assumption of a plane wave incident at the base of the crust may not be valid.

For all three models the contour maps of reflection coefficients are similar in nature. Within the frequency range shown (0–0.45 cps), the values are consistently high for angles below 15 degrees; beyond that the variations differ. While the contours for an oceanic U. S. crust show a repeating pattern, with bands of high value at several frequencies for all the angles, those for Peru-Altiplano and central U. S. models are lacking in regularity. The contour map for the thicker Peru-Altiplano crust also shows a more rapid change than the central U. S. crust; this is expected from the fact that the reflection coefficient from a layered crust is actually scaled by the dimensionless parameter formed by a combination of k, H_j and sin i; where k is

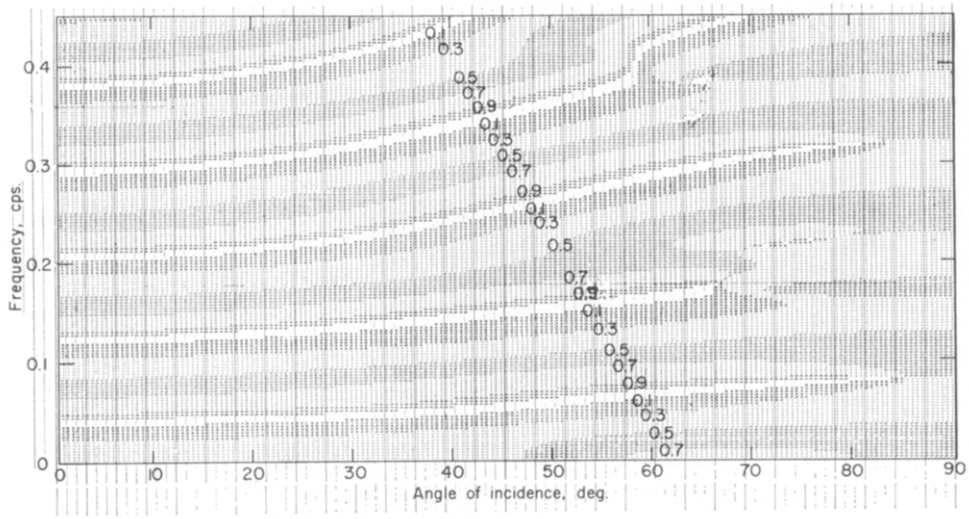

FIG. 6. Phase shifts (fraction of a circle) at the base of the crust for average central U. S. structure.

the wave number, H_j the thickness of the layer, i the incidence angle (Fernandez, 1965).

The local minimums on the contour maps are the places where most of the incident P wave energy is converted to shear wave energy. Similarly, the local highs are the places where a relatively small amount of energy is converted to shear energy upon reflection.

The phase-shift plots (Figures 4 and 5) have the same scaling phenomenon. The two continental models showed essentially the same feature, and we therefore omit the one for Peru-Altiplano structure.

Synthesized Records. Fourier synthesis was employed to transform to the time domain the frequency-dependent complex Fourier spectrum computed by Haskell's method for several angles of incidence for a flat frequency spectrum (Fourier transform of $\delta(t)$) input. Synthesized records enable us to gain some insight as to what happens to the wave after its impingement on the bottom of the crust. The complex spectrums were multiplied by the response of a simulated 30–100 instrument to suppress ultra-long period components for better synthesis and for comparison with the seismograms recorded by USCGS world-wide net seismometers.

The synthesized records for several angles of incidence for the three models mentioned in a previous section are presented in Figures 7, 8 and 9. The bottom two traces in Figures 7 and 9 are what the seismograms would appear to be for an instrument located on a continent having the average central U. S. structure.

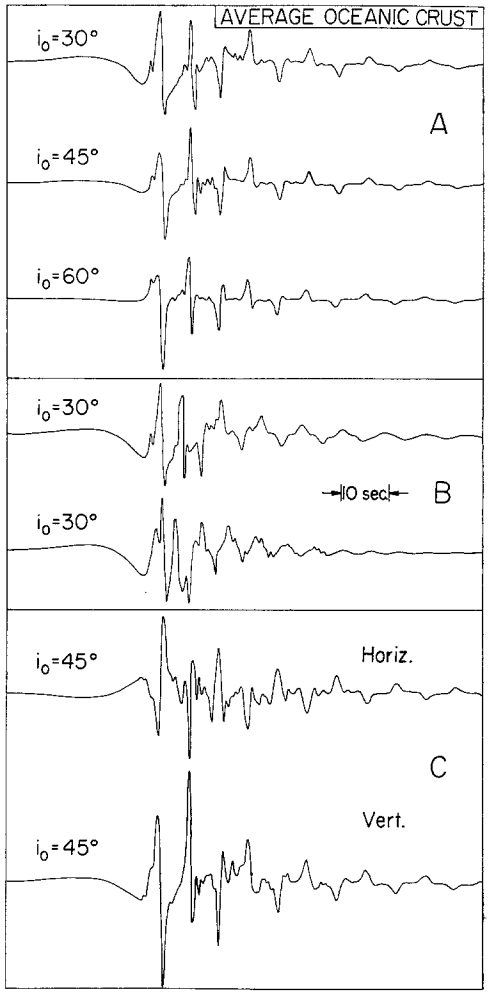

FIG. 7. Synthesized records for average oceanic structure. (A) At the base of the crust for the downgoing reflected wave near the point of reflection. (B) At the base of the crust with water layer thickness decreased to 3 km for upper trace and to 2 km for lower trace. (C) Reflected wave transmitted through an average central U. S. structure.

(Namely, the crustal transmission response at the receiving station was multiplied to the spectrum described above before synthesizing.) The others illustrate the crustal effects at the point of reflection for different models. Comparing these two categories of the synthesized traces, it is evident that the salient features of the incident wave at the bottom of the crust under the receiver are preserved; oscillations corresponding to reflections at interfaces during transmission through the crust are added to the incident wave.

The reflected waves from an oceanic crust (Figure. 7) are rather complicated owing to the multiple reflections set up in the water layer by the incident wave. The later arrivals are repeated at a constant interval; this interval is approximately equal to the vertical two-way travel time for a P wave in the water layer. This results from the fact that the contrast between the P wave velocity in the half-space and that in the water is so great, for the angles of incidence considered, the ray path is close to the normal in the water layer, and, hence, the travel time approaches that for vertical transit. Notice also the polarity is changed for every successive arrival, due to the π phase change occuring at the free surface. The amplitude of the later arrivals decrease as time goes on as a result of the energy being transmitted through the ocean

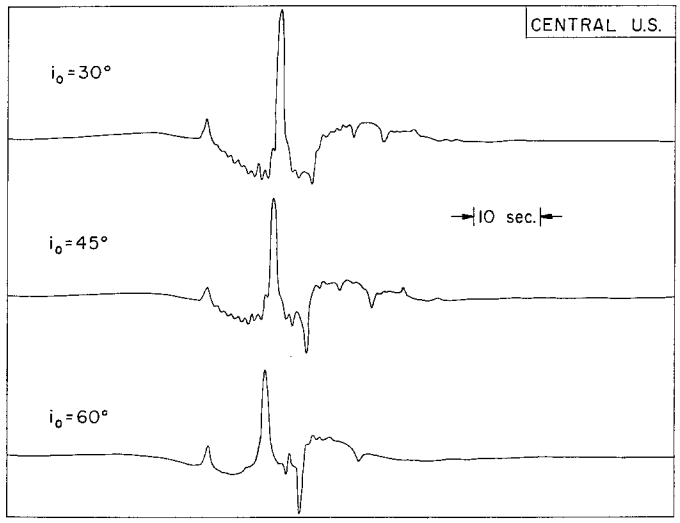

FIG. 8. Synthesized records for central U. S. structure.

bottom or converted to other wave types at each reflection from the bottom of the ocean. As the ocean depth decreases the intervals between the individual arrivals decrease; for a two thousand meter deep ocean they are no longer distinguishable. This is demonstrated in Figure 7; in box B, the water depth was decreased from 4.5 km to 3 km for the upper trace and to 2 km for the lower trace. The continental reflections (Figures 8 and 9) are quite different in appearance from the oceanic counterpart. The clearly isolated first arrival, appearing immediately after the incident wave hits the crust, is the reflection from the base of the crust. The main signal following it corresponds to the reflection from the free surface. The time lag between the initial disturbance and main pulse depends on the total thickness of the crust and velocity distribution in the crust; the difference in time lag accounts for the main difference between two groups of synthesized records—those for a "thick" Peru-Altiplano crust and those for a relatively thin average central U. S. structure. In contrast to oceanic reflections very little energy is trapped in the layered system; the record is therefore fairly clean. Based on these observations, it appears that for the sole purpose of determining whether the reflection occurred under the continent or in the ocean the pulse shape of PP wave is a good indicator.

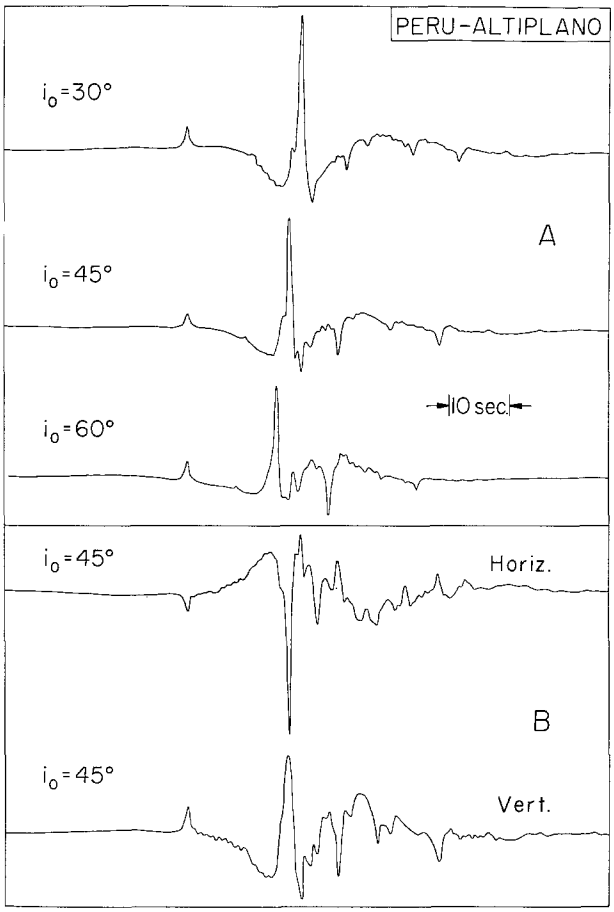

FIG. 9. Synthesized records for Peru-Altiplano structure. (A) At the base of the crust. (B) Reflected wave transmitted through an average central U. S. structure.

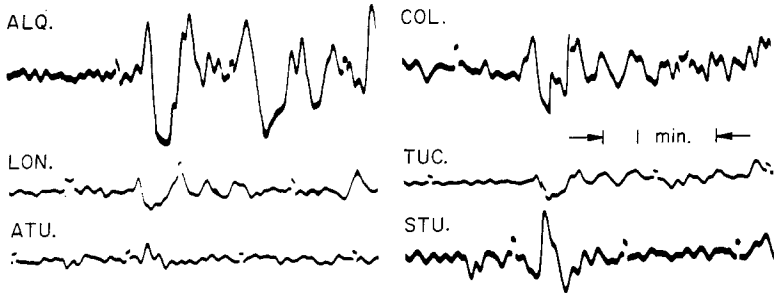

FIG. 10. Sample WWNSS seismograms from Banda Sea shock of March 27, 1964.

DISCUSSION AND CONCLUSION

Several authors (Mei, 1943, Papazachos, 1964) advanced the conclusion from their data reduction under various assumptions that some of the main reflections must have occurred at the base of the crust rather than at the free surface. The synthe-

sized records reveal quite clearly this could hardly be the case. Physically, reflection from an interface would be at its strongest when the acoustic impedance mismatch is the greatest between the two media in contact; such a situation invariably occurs at the earth's surface.

A number of observations were made of *PP* on actual seismograms. Good *PP* pulses could usually be found on records for very shallow or very deep earthquakes at distances such that *PP* is well isolated. In order to see how realistic our theory is, we have compared the synthesized traces to sample seismograms from March 21, 1964, Banda Sea shock on which *PP* could be easily identified. They are shown in Figure 10. The earthquake occurred at a depth of 350 km and had a magnitude of $6\frac{1}{2}$. Perusal of travel time curves by Gutenberg and Richter (1936) shows that between epicentral distances of 70 and 125 degrees *PP* waves would in general be isolated from other arrivals, one minute before and one minute after the arrival. In

TABLE 2

LOCATIONS, EPICENTRAL DISTANCES OF THE STATIONS AND THE GEOGRAPHICAL POINTS OF REFLECTION FOR *PP* PERTAINING TO FIGURE 10

	Location	Δ(°)	Point of Reflection
ALQ	Albuquerque, New Mexico, U. S. A.	122.6	Pacific Ocean
ATU	Athens, Greece	105.1	Northern India
COL	College, Alaska, U. S. A.	93.3	Pacific Ocean
LON	Longmire, Washington, U. S. A.	108.5	Pacific Ocean
STU	Stuttgart, Germany	113.5	Western China
TUC	Tucson, Arizona, U. S. A.	119.8	Pacific Ocean

the figure we have given the station abbreviations for each long-period WWNSS record; epicentral distances and the geographical locations of the points of reflection are listed in Table 2. We can clearly discern the relatively simple nature of the STU and ATU records with points of reflection under the continent as contrasted with other traces with points of reflection in the Pacific ocean. This is consistent with the conclusion we reached previously. We must remember, however, that the submarine topography in the case of oceanic reflections and the land topography in the case of continental reflections can modify the pulse shape considerably when the wavelength we are observing is commensurate with the dimension of the topographical features. Further examples, mostly recorded by short-period instruments, can be found in the work by Gutenberg and Richter (1935).

When both *P* and *PP* are clear on a single seismogram the crustal reflection transfer function can be found within a constant factor under certain assumptions. Let

$$P(\omega) = F(\omega)T(\omega, i_p) \exp\left[-\int_{c_1} \gamma(\omega)\, ds\right]$$

where $F(\omega)$ is the source spectrum, $T(\omega, i_p)$ is the crustal transmission transfer function at the receiver for angle of incidence i_p, $\gamma(\omega)$ is the absorption coefficient for the *P* wave and the integration is carried out along the ray path C_1. Similarly

$$PP(\omega) = \beta F(\omega) R(\omega) T(\omega, i_{pp}) \exp\left[-\int_{c_2} \gamma(\omega)\, ds\right],$$

β being the amplitude ratio, assumed to be independent of frequency. Then

$$R(\omega) = \frac{PP(\omega)}{\beta P(\omega) A(\omega)},$$

where

$$A(\omega) = \exp\left[-\left[\int_{c_2} \gamma(\omega)\, ds - \int_{c_1} \gamma(\omega)\, ds\right]\right] \frac{T(\omega, i_{pp})}{T(\omega, i_p)}.$$

$T(\omega, i)$ can be calculated by Haskell's method, $\gamma(\omega)$ has been determined by Anderson and Julian (1965) and Teng (1965). PP travels through the upper mantle and the crust, where the attenuation is high, two more times than P does, so the high frequencies would be relatively more attenuated in PP than in P. The factor β can also be eliminated if we work out the radiation pattern of the source (Ben-Menahem *et al*, 1965, and Teng and Ben-Menahem, 1965).

It should be noted that the computations in this paper did not take into account either the curvature of the earth or the curvature of the wave front. The problem of reflected waves in a liquid sphere was treated by Jeffreys and Lapwood (1957), Burridge (1962) and Alterman and Kornfeld (1965) and in a solid sphere by Burridge (1963). One of the conclusions they reached is that for PP waves that correspond to stationary time paths the pulse shape is related to the P pulse as the Fourier integral is related to the Allied-Fourier integral. Thus if the source function is $\delta(t)$ the PP pulse will appear as $\delta'(t)$. Detailed discussion is given in Burridge (1963). The spherical effect can be incorporated into the result obtained in the present work if the phenomenon should become salient in the frequency range under observation.

We see that PP/P is a function of frequency and depends not only on the structure at the point of reflection but also on the radiation pattern of the source, structure at the receiver and the absorption of waves while propagating along specific paths. Only after these factors are isolated can we recover the spectral properties of the crust at the point of reflection.

If a dependable spectral response $R(\omega)$ of the crust can be obtained from seismograms, then it can be used to determine the structure at the point of reflection to a much higher order of accuracy than the single amplitude ratio PP/P. With the establishment of large seismic arrays, which make possible the effective enhancement in signal to noise ratio, this procedure may become practical in the near future.

Acknowledgments

The authors wish to thank Dr. D. L. Anderson for discussions at various stages of the work. Mr. T. L. Teng assisted the authors by lending his collection of seismograms for Banda Sea shocks. We would also like to acknowledge the assistance of Mr. Laszlo Lenches in the preparation of graphical material.

This research was supported by the Advanced Research Projects Agency and was monitored by the Air Force Office of Scientific Research under Contract AF-49(638)-1337.

References

Aki, K. (1960). Study of earthquake mechanism by a method of phase equalization applied to Rayleigh and Love waves, *J. Geophys. Res.* **64,** 729–740.

Alterman, Z. and P. Kornfeld (1965). Shallow focus explosion in a liquid sphere, *J. Roy. Astro. Soc.*, **9,** 121–152.

Anderson, D. L. and B. R. Julian (1965). Travel times, velocities and amplitudes of body phases, Abstract of papers submitted to the annual meeting of the Seism. Soc. Am. 1965.

Ben-Menahem, A., S. W. Smith and T. L. Teng (1965). A procedure for source studies from spectrums of long-period seismic waves, *Bull. Seism. Soc. Am.* **55,** 203–235.

Brekhovskikh, L. M. (1960). *Waves in layered media,* Academic Press, New York.

Burridge, R. (1962). The reflexion of high-frequency sound in a liquid sphere, *Proc. Roy. Soc. London, A*, **270,** 144–154.

Burridge R. (1963). The reflexion of a pulse in a solid sphere, *Proc. Roy. Soc. London, A*, **276,** 367–400.

Byerly, Perry, Alexis I. Mei, S.J. and Carl Romney (1949). Dependence on azimuth of the amplitudes of *P* and *PP*, *Bull. Seism. Soc. Am.* **39,** 269–284.

Dorman, J. (1962). Period equation for waves of Rayleigh type on a layered, liquid solid half-space, *Bull. Seism. Soc. Am.* **52,** 389–397.

Fernandez, L. M. (1965). The determination of crustal thickness from the spectrum of the *P* wave, *Doctoral Dissertation,* St. Louis University.

Gutenberg, B. and C. F. Richter (1935). On seismic waves, (2nd paper), *Gerlands Beitr. Geophys.* **45,** 280–360.

Gutenberg, B. and C. F. Richter (1936). Unpublished charts with data taken from "Materials for the studies of deep-focus earthquakes," *Bull. Seism. Soc. Am.* **26,** 341–390.

Gutenberg, B. (1944). Energy ratio of reflected and refracted seismic waves, *Bull. Seism. Soc. Am.* **34,** 85–102.

Harkrider, D. G. (1964a). Propagation of acoustical gravity waves from an explosive source in the atmosphere, Part I. of *Thesis,* California Institute of Technology.

Harkrider, D. G. (1964b). Surface waves in multilayered elastic media, 1. Rayleigh and Love waves from buried sources in a multilayered elastic half-space, *Bull. Seism. Soc. Am.* **54,** 627–679.

Haskell, N. A. (1953). The dispersion of surface waves on multilayered media, *Bull. Seism. Soc. Am.* **43,** 17–34.

Haskell, N. A. (1960). Crustal reflection of plane *SH* waves, *J. Geophys. Res.* **65,** 4147–4150.

Haskell, N. A. (1962). Crustal reflection of *P* and *SV* waves, *J. Geophys. Res.* **67,** 4751–4767.

Jeffreys, H. and E. R. Lapwood (1957). The reflexion of a pulse within a sphere, *Proc. Roy. Soc.* (London) A, **241,** 455–479.

McEvilly, T. V. (1964). Central U.S. crust—upper mantle structure from Love and Rayleigh wave phase velocity inversion, *Bull. Seism. Soc. Am.* **54,** 1997–2015.

Mei, A. I., S.J. (1943). The amplitude ratio *PP/P* as recorded by Galizin seismographs, *Bull. Seism. Soc. Am.* **33,** 149–196.

Papazachos, B. (1964). Angle of incidence and amplitude ratio of *P* and *PP* waves, *Bull. Seism. Soc. Am.* **54,** 105–121.

Raitt, R. W. (1963). *The Crustal Rocks, in "The Sea"*, edited by M. N. Hill, Interscience Publishers, pp. 85–102.

Steinhart, J. S. and R. P. Meyer (1961). *Explosion studies of continental structure,* Carnegie Inst. Wash., Publication 622.

Teng, T. L. and A. Ben-Menahem (1965). Mechanism of deep earthquakes from spectrums of isolated body-wave signals, 1. The Banda Sea Earthquake of March 21, 1964, *J. Geophys. Res.* **70,** 5157–5170.

Teng, T. L. (1965). *Amplitudes of body waves*, Technical Report Contract AF-49(638)-1337.
Thomson, W. T. (1950). Transmission of elastic waves through a stratified solid medium, *J. Appl. Phys.* **21**, 89–93.

Seismological Laboratory
California Institute of Technology
Pasadena, California
(Division of Geological Sciences, Contribution No. 1382)

Manuscript received September 28, 1965.